

Free Vibration Analysis of Perforated Plates Using Equivalent Elastic Properties

**Suhn Choi, KyeongHoon Jeong, TaeWan Kim,
KangSoo Kim, and KeunBae Park**

Korea Atomic Energy Research Institute
150 Dukjin-dong, Yusong-gu, Taejon 305-353, Korea

(Received October 27, 1997)

Abstract

Many studies for the perforated plates have been done, especially on the subject of static behavior and stress distribution in the plate. Equivalent elastic properties are one of the successive concepts for this problem. However little effort was taken to get their dynamic characteristics.

In this paper finite element modal analysis was performed for the perforated plates having square and triangular hole patterns. An attempt to use existing equivalent elastic properties into the modal analysis of the plate was carried out. To verify feasibility of the finite element models, modal test was also performed on one typical perforated plate. System parameters such as natural frequencies and mode shapes were extracted and compared with the analysis results.

1. Introduction

Perforated plates and shells are one of the most commonly and widely used structural components in many engineering applications. In nuclear reactors there are several perforated structures which provide both structural support and flow-passage of a coolant. It is required that these structures shall withstand various external loadings such as dynamic loading from an earthquake and loading due to design basis pipe break, thus shall ensure the structural integrity.

Many attempt have been made to get an understanding of stress-strain state of a plate having many holes. Recently development of large computer and finite element technique enables to

analyze these perforated plate problems into relatively real fashion. However fine meshing due to existence of many holes makes it very costly and time and labor consuming.

Using elasticity theory O' Donnell[1] has suggested equivalent elastic properties in 1970 that make the solid plate deflection be identical to that of the real plate. During the last decades many authors[2,3,4] have proposed experimental or theoretical methods to solve perforated plate problem, which lead to a great disparity of values. Osweiler[2] has summarized these concepts in his paper and suggested sets of curves which are incorporated in French CODAP code[5]. However, most of the efforts have been given to static stress-strain problems. In 1982 Plyat and

Villasor of Westinghouse[6] evaluated the feasibility of equivalent elastic properties to vibration problems of plates with certain boundary conditions and geometry.

In this paper the concept of equivalent elastic properties for solving vibration problem of a thin, rectangular, free-edged perforated plate is evaluated with finite element analyses and experiment. The effect of the ligament efficiency on the natural frequencies are also investigated.

2. Theory of Plate

2.1. Vibration of Solid Rectangular Plate

The governing equation for a plate motion is given in equation (1) [7] :

$$-D \nabla^4 w = \rho \frac{\partial^2 w}{\partial t^2}, \quad D = \frac{E h^3}{12(1-\nu^2)} \quad (1)$$

$$\text{where } \nabla^4 = \frac{\partial^4}{\partial x^4} + 2 \frac{\partial^4}{\partial x^2 \partial y^2} + \frac{\partial^4}{\partial y^4}$$

After separation of variables with $w = W \cdot f$, where W depends on the spatial coordinates only and f is a time-dependent harmonic function of frequency ω , equation of motion in rectilinear coordinates becomes :

$$D \nabla^4 W = \omega^2 \rho W \quad \text{or} \quad \nabla^4 W(x, y) - \beta^4 W(x, y) = 0, \quad \beta^4 = \frac{\omega^2 \rho}{D} \quad (2)$$

Boundary conditions for the free edge are given from the fact that the moment and Kelvin-Kirchoff edge reaction are zero :

$$\nabla^2 W - (1-\nu) \left(\frac{1}{R} \frac{\partial W}{\partial n} + \frac{\partial^2 W}{\partial s^2} \right) = 0, \quad (3-1)$$

$$\frac{\partial}{\partial n} \nabla^2 W + (1-\nu) \frac{\partial}{\partial s} \left(\frac{\partial^2 W}{\partial n \partial s} - \frac{1}{R} \frac{\partial W}{\partial s} \right) = 0$$

Since $R \rightarrow \infty$ for the rectangular plate, above equation will be

$$\nabla^2 W - (1-\nu) \frac{\partial^2 W}{\partial s^2} = 0, \quad (3-2)$$

$$\frac{\partial}{\partial n} \nabla^2 W + (1-\nu) \frac{\partial^3 W}{\partial n \partial s^2} = 0$$

Solving equation (2) the general solution is given by

$$W(x, y) = A_1 \sin \alpha x \sin \gamma y + A_2 \sin \alpha x \cos \gamma y + A_3 \cos \alpha x \sin \gamma y + A_4 \cos \alpha x \cos \gamma y + A_5 \sinh \alpha_1 x \sinh \gamma_1 y + A_6 \sinh \alpha_1 x \cosh \gamma_1 y + A_7 \cosh \alpha_1 x \sinh \gamma_1 y + A_8 \cosh \alpha_1 x \cosh \gamma_1 y, \quad (4)$$

$$\alpha^2 + \gamma^2 = \alpha_1^2 + \gamma_1^2 = \beta^2$$

Natural frequency of a rectangular solid plate is given by the following formula [8] :

$$\omega_{ij} = \frac{\lambda_{ij}^2}{2 \pi a^2} \left[\frac{E h^3}{12 \gamma (1-\nu^2)} \right]^{1/2} \quad (5)$$

where a : length of plate, h : thickness, γ : mass per unit area, and λ_{ij} is a coefficient for modes and boundary conditions. And corresponding natural modes are

$$W_{mn}(x, y) = A_{mn} \cos \frac{m\pi x}{a} \cos \frac{n\pi y}{b} \quad (6)$$

2.2. Equivalent Elastic Plate

In order to account for the weakening effect of the holes, the flexural rigidity D of the plate before drilling is reduced by a factor η , called its 'deflection efficiency', which allows to calculate the flexural rigidity, D^* , of the equivalent plate :

$$D^* = \eta \cdot D \quad (7)$$

The deflection efficiency η must be determined such as the equivalent solid plate deflection be identical to that of the real plate. Using elasticity theory O' Donnell[1,9] has shown that it is possible to determine the value η satisfying this condition. η depends on the type of penetration

Table 1. Deflection Efficiency Factor

r	Triangular pattern			Square pattern		
	E*/E	ν^*	density ratio*	E*/E	ν^*	density ratio*
0.1	0.132	0.409	0.452	0.188	0.247	0.427
0.2	0.265	0.241	0.567	0.315	0.168	0.548
0.5	0.659	0.221	0.831	0.665	0.209	0.823

*density ratio = (weight of perforated plate) / (weight of solid plate)

pattern and on the degree of holes of the plate, represented by its ligament efficiency defined as :

$$r = \frac{p-d}{p} ; p = \text{pitch}, d = \text{hole diameter} \quad (8)$$

Once D^* has been calculated, the classical equations of solid plates allow to calculate the stresses in the equivalent plate and then in the real plate in a reverse manner.

O' Donnell proposed a single set of curves for in-plane and bending loading in order to determine E^*/E and ν^* as a function of ligament efficiency for triangular and square hole patterns. Detail theoretical derivations can be found in references 1 and 9.

Values of the deflection efficiency factor used in this study are taken from reference 2 and shown in Table 1.

3. Finite Element Analysis

Two kinds of models are generated to verify the adequacy of the equivalent plate concept in the modal analysis of perforated plates. The first model is the finite element plate model having actual holes in it, and the second one is the plate having equivalent elastic properties. By comparing natural frequencies of the same mode between perforated and solid model the concept of equivalent plate can be justified to be used in modal analysis of perforated plate.

With these models finite element analysis was

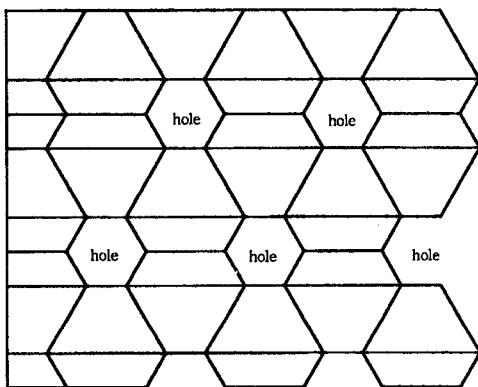
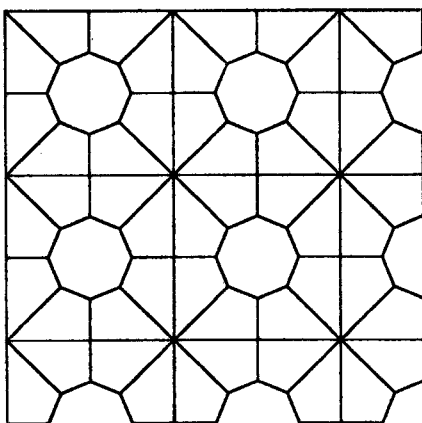
performed to get natural frequencies and mode shapes. General purpose finite element code ANSYS was chosen to be an analysis tool. Three analyses models were generated for both triangular and square hole patterns. Ligament efficiency (r) was chosen to be a typical value, 0.1, 0.2, and 0.5. Figure 1 and 2 show the typical finite element models used in this study. Geometry and dimension for the models are taken with arbitrary numbers. However the thickness to pitch ratio is set to 0.25. Plate dimension of $l \times w \times t$ in Table 2 for triangular and square hole pattern is decided to be used. Due to mesh problem the holes are modeled as octagonal shape or hexagonal shape as seen in the figures. This will not make a considerable effect on the global vibrational behavior of a perforated plate.

Subspace iteration option to extract eigenvalues is used for the analysis. Each eigenvalue is classified into mode description by reviewing mode shapes. Four-node shell element (STIF63) is used because it also gives accurate eigenvalues for plate and shell problems.

Equivalent plate is merely a solid plate having equivalent elastic properties such as elastic modulus, Poisson's ratio, and density. Plates are assumed to have isotropic, homogeneous elastic properties taken from reference 2. Models are equally rectangular meshed into 200 elements. Basic material properties are taken as $E = 30 \times 10^6$ psi, density = 0.29 lbs/in³, $\nu = 0.3$.

Table 2. Dimension of the Finite Element Plate Model

	Pitch	η	Length	Width	Thickness
Triangular	2.0	0.1	20.9	33.082	0.5
	2.0	0.2	20.8	33.255	0.5
	2.0	0.5	20.5	33.775	0.5
Square	2.0	0.1/0.2/0.5	20.0	40.0	0.5

**Fig. 1. Finite Element Model of the Perforated Plate with the Triangular Penetration Pattern****Fig. 2. Finite Element Model of the Perforated Plate with the Square Penetration Pattern**

4. Experimental Modal Analysis

4.1. Test Setup

To verify the analysis method and FE model used, typical modal test was performed for the plate with triangular penetration pattern.

Measurement setup for typical modal experiment is shown in Figure 3 : system consists of one input and one output sensor, conditioning amplifiers, digital data acquisition system of sampling capability, 2 channel FFT analyzer, and auxiliary devices such as oscilloscope and data backup device.

Vibratory motion is taken with a piezo-electric type accelerometer, while the excitation is given by an impulse hammer. Manipulating auto power spectrum of input and output, and their cross power spectrum, FRF (frequency response function) can be obtained. And from the peak values of FRF mode shape can be drawn.

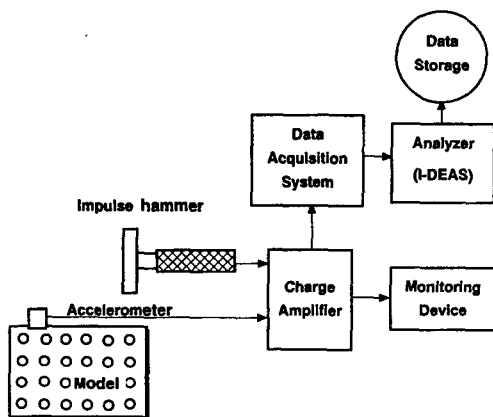
In this study just a single plate was used in a modal test. Free edge condition is chosen to be a test boundary condition, since it is not easy to obtain simply supported and/or fixed edge. To obtain the free boundary condition a target plate was suspended by a string. A piezoelectric type accelerometer and an impulse hammer together with a charge amplifier are installed for sensing input and output vibration signals. Measurement data is monitored on-line by an oscilloscope, and is stored on a magnetic tape for future usage. Data

Table 3. Comparison of Natural Frequencies from FEM Analysis and Test

Mode	FEM	Fadj. ^{*1}	Ftest	Dev. ^{*2}	Mode	FEM	Fadj. ^{*1}	Ftest	Dev. ^{*2}
(1,3)	55.4	50.28	50.28	100	(3,4)	404.7	367.32	369.62	99.4
(3,2)	183.7	166.73	167.36	99.6	(1,6)	507.3	460.44	450.70	102.2
(3,3)	273.4	248.15	258.76	95.9	(4,3)	524.1	475.69	480.23	99.1
(1,5)	308.5	280.01	273.11	102.5	(3,5)	570.3	517.62	512.47	101.0

*1. Fadj. = Adjusted freq. with respect to the 1st. mode between analysis and test.

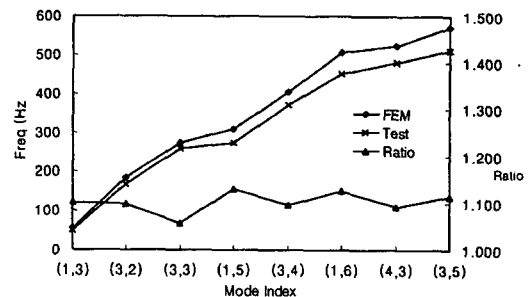
*2. Dev. = Ratio of Fadj./Ftest

**Fig. 3. Schematic Diagram of Modal Test Setup**

acquisition system with I-DEAS TEST software is set for signal processing.

4.2. Data Processing

To get mode shapes of a plate updating method of single accelerometer movement is utilized : an accelerometer changes its measuring point from one node to another while impulse hammer provide the excitation to a certain fixed node. Measurements are done for total 30 points (6×5 node grid) over the model plate. Data acquisition (sampling and A/D conversion) is performed using HP data logger. I-DEAS TEST module is used as an analysis tool for measured vibration signals.

**Fig. 4. Comparison of Test and FEM Results**

Sampling frequency range is set to 0-1600 Hz so that one can get the meaningful result upto 800 Hz. Number of averages on the signal is taken 3 after seeing a pretest result which is very clear and sharp showing its low noise, lightly damped system. Frequency response function H1 and coherence are the main results from this test. Since the excitation is given by impact, rectangular and exponential windows are applied to input and output signals, respectively.

Natural Frequencies are picked by multi-reference method. After reviewing mode shapes the natural frequencies are classified following mode index (i, j).

5. Results and Discussions

In Table 3 and figure 4 given are the comparison of natural frequencies from finite

Table 4. Natural Frequencies of a Plate with Triangular Hole Pattern

Mode	Perforated FEM			Equivalent Plate FEM		
	0.1	0.2	0.5	0.1	0.2	0.5
(1,1)	76.8	81.7	89.1	48.6	65.0	85.2
(0,2)	83.8	83.9	86.8	51.2	63.7	80.4
(1,2)	176.7	186.3	201.8	112.9	147.2	191.4
(2,0)	177.0	193.7	233.7	136.7	166.3	222.1
(2,1)	225.3	263.5	300.4	176.3	214.6	283.2
(0,3)	-	229.7	239.3	139.2	175.3	221.9
(1,3)	330.7	342.6	365.5	209.8	266.6	343.2
(2,2)	384.4	403.0	441.9	249.0	319.4	418.1

Table 5. Natural Frequencies of a Plate with Square Hole Pattern

Mode	Perforated FEM			Equivalent Plate FEM		
	0.1	0.2	0.5	0.1	0.2	0.5
(0,2)	52.0	55.1	61.3	42.8	48.8	57.9
(1,1)	76.3	76.9	78.4	54.1	63.7	74.3
(0,3)	143.5	152.1	169.9	118.6	135.0	160.3
(1,2)	162.9	165.3	171.4	118.5	138.5	162.2
(2,0)	207.7	220.7	249.0	174.0	196.7	234.3
(2,1)	258.6	270.1	296.8	206.7	235.5	279.4
(1,3)	272.2	279.0	295.1	204.7	236.9	278.9
(0,4)	282.2	299.5	336.9	235.3	266.0	316.9

analysis and test. The results are agreed well within 4% deviation. This shows that the finite element analysis can be a good method of predicting dynamic characteristics of a perforated plate.

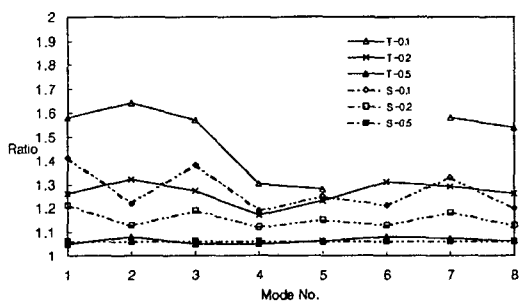
The natural frequency results from the finite element analysis for the various ligament shapes are given in Table 4 and 5. Natural frequencies for the plates with triangular hole patterns ($r = 0.1, 0.2, 0.5$) and their equivalent plates are given in Table 4. In Table 5 natural frequencies for the plates with square hole patterns and their equivalent plates are given. As holes become larger, the stiffness drops more rapid than mass, and this gives a frequency drop in all modes. As is the same for the triangular patterns, the natural

frequencies also drop for the square pattern. However, the numerical difference of the square pattern between 'perforated' and 'equivalent' is smaller than the triangular pattern. In Table 6 and figure 5 ratio of natural frequencies for 'perforated' to 'equivalent' is given. As shown in the graph the frequency ratio remains quite stable along modes for a certain ligament efficiency ratio, r . However the deviation is getting higher as r increases. This indicate that the equivalent property E^*/E from reference 2 may be underestimated with respect to the calculation of dynamic characteristic for larger penetration case.

Dynamic modification constant to static E^*/E and ν^* can be proposed, since the ratios in any column of a ligament efficiency (r) remain stable

Table 6. Natural Frequencies Ratios of Perforated Plates

Mode	Triangular pattern			Square Pattern		
	0.1	0.2	0.5	0.1	0.2	0.5
(1,1)	1.58	1.26	1.05	1.41	1.21	1.06
(0,2)	1.64	1.32	1.08	1.22	1.13	1.06
(1,2)	1.57	1.27	1.05	1.38	1.19	1.06
(2,0)	1.30	1.17	1.05	1.19	1.12	1.06
(2,1)	1.28	1.23	1.06	1.25	1.15	1.06
(0,3)	-	1.31	1.08	1.21	1.13	1.06
(1,3)	1.58	1.29	1.07	1.33	1.18	1.06
(2,2)	1.54	1.26	1.06	1.20	1.13	1.06

**Fig. 5. Frequency Deviation between Perforated Plate and Equivalent Plate**

meaning linear nature of this phenomena.

6. Conclusions

The concept of the equivalent solid plate elaborated for solving stress-strain problems of perforated plates can be used as an approximation in the modal analysis of similar plates with free boundaries. However, to obtain sufficiently accurate results, care must be taken to determine the proper equivalent elastic properties (E^*/E and ν^*) which may be different from the values for static problem. The difference of equivalent elastic properties from static problem is thought to become significant as the ligament efficiency value gets smaller.

As previous studies[1,2] on stress-strain state of the perforated plates indicated that thickness is also a key parameter for determining E^*/E and ν^* ; plates can be classified as thin, medium, and thick plate according to its thickness, this study need to be extended to include more parameters including boundary condition and thickness.

Acknowledgement

It is acknowledged that the experiment of this study is supported by Mr. J.H.Park, Dr. T.R.Kim of KAERI Vibration Lab. and Dr. M.K.Chung of KAERI Thermal Hydraulic Division.

References

1. Slot, T. and O' Donnell, N.J., "Effective Elastic Constants for Thick Perforated Plates with Square and Triangular Penetration Patterns", J. of Engineering for Industry, ASME Trans., Series B., pp 935-942 (1971)
2. Osweiller, F., "Evolution and Synthesis of the Effective Elastic Constants Concept from 1948 to Present - New Design Curves for Triangular and Square Patterns", PVP-Vol.120 (1987)
3. Horvay, "The Plane-stress Problem of Perforated Plates", J. of Applied Mechanics,

- Vol.17 ; Trans-ASME, Vol. 74 (1952)
4. Slot, T., "Stress Analysis of Thick Perforated Plates", Technical publication, Westport, CT, USA. (1972)
 5. CODAP- Code Francais de Construction des Appareils a Pression-Edition 1985 (1985)
 6. Plyat, S.N. and Villasor, A.P.Jr., "Modal Analysis of Perforated Plates with Triangular patterns of Circular Holes", Proc. of the 1st Int'l Modal Anal. Conf., November, pp 326-332 (1982)
 7. Meirovitch, L., *Analytical Methods in Vibrations*, The MacMillan Co.(1971)
 8. Blevins, R. D., *Formulas for Natural Frequency and Mode Shape*, Van Nostrand Reinhold Co. (1979)
 9. O' Donnell, N.J., "Effective Elastic Constants for the Bending of Thin Perforated Plates with Triangular and Square Penetration Patterns", J. of Engineering for Industry, ASME Trans., Series B., pp 121-128 (1973)